

Supplementary information

Long-Chain Amine-Templated Synthesis of Gallium Sulfide and Gallium Selenide Nanotubes[†]

A. Seral-Ascaso,^{a,b} S. Metel,^{a,c} A. Pokle,^{a,b} C. Backes,^{a,b} C. J. Zhang,^{a,c} H. C. Nerl,^{a,b} K. Rode,^{a,b} N. C. Berner,^{a,c} C. Downing,^a N. McEvoy,^{a,c} E. Muñoz,^d A. Harvey,^{a,b} Z. Gholamvand,^{a,b} G. S. Duesberg,^{a,c} J. N. Coleman^{a,b} and V. Nicolosi^{a,b,c}

^a CRANN & AMBER, Trinity College Dublin, Pearse Street, Dublin 2, Ireland

^b School of Physics, Trinity College Dublin, College Green, Dublin 2, Ireland

^c School of Chemistry, Trinity College Dublin, College Green, Dublin 2, Ireland

^d Instituto de Carboquímica ICB-CSIC, Miguel Luesma Castán 4, 50018 Zaragoza, Spain

Supplementary information

Index

Figure S1. TEM micrographs of A_tGaS_x -NTs and A_tGaSe_y -NTs	Page 3
Figure S2. EDX (TEM) spectra of A_tGaS_x -NTs and A_tGaSe_y -NTs	Page 4
Figure S3. EDX (SEM) mapping of the elements distribution on the A_tGaS_x -NTs	Page 5
Figure S4. TGA curve of A_tGaS_x -NTs and A_tGaSe_y -NTs	Page 6
Figure S5. EDX and XRD of the TGA residues of A_tGaS_x -NTs and A_tGaSe_y -NTs	Page 7
Figure S6. TXRF spectra of A_tGaS_x -NTs and A_tGaSe_y -NTs	Page 8
Figure S7. XPS survey of A_tGaS_x -NTs and A_tGaSe_y -NTs	Page 9
Figure S8. XPS of N1s, Ga3d, S2p and Se3d of A_tGaS_x -NTs and A_tGaSe_y -NTs	Page 10
Figure S9. SEM of ageing study of A_tGaSe_y -NTs	Page 11
1. Synthesis optimization of the nanotubes	Page 12
1.1- Optimization of A_tGaS_x -NTs	Page 12
Table 1. Synthesis conditions for A_tGaS_x -NTs	Page 14
Figure S10. SEM micrographs of A_tGaS_x -NTs	Page 15
1.2- Optimization of A_tGaSe_y -NTs	Page 16
Table 2. Synthesis conditions for A_tGaSe_y -NTs	Page 17
Figure S11. SEM micrographs of A_tGaSe_y -NTs	Page 18
1.3- Amine-templated gallium telluride nanotubes synthesis studies	Page 19
Table 3. Synthesis conditions in the gallium-tellurium system	Page 20
Figure S12. SEM micrographs, EDX and XRD of the obtained materials	Page 21
2- References	Page 22

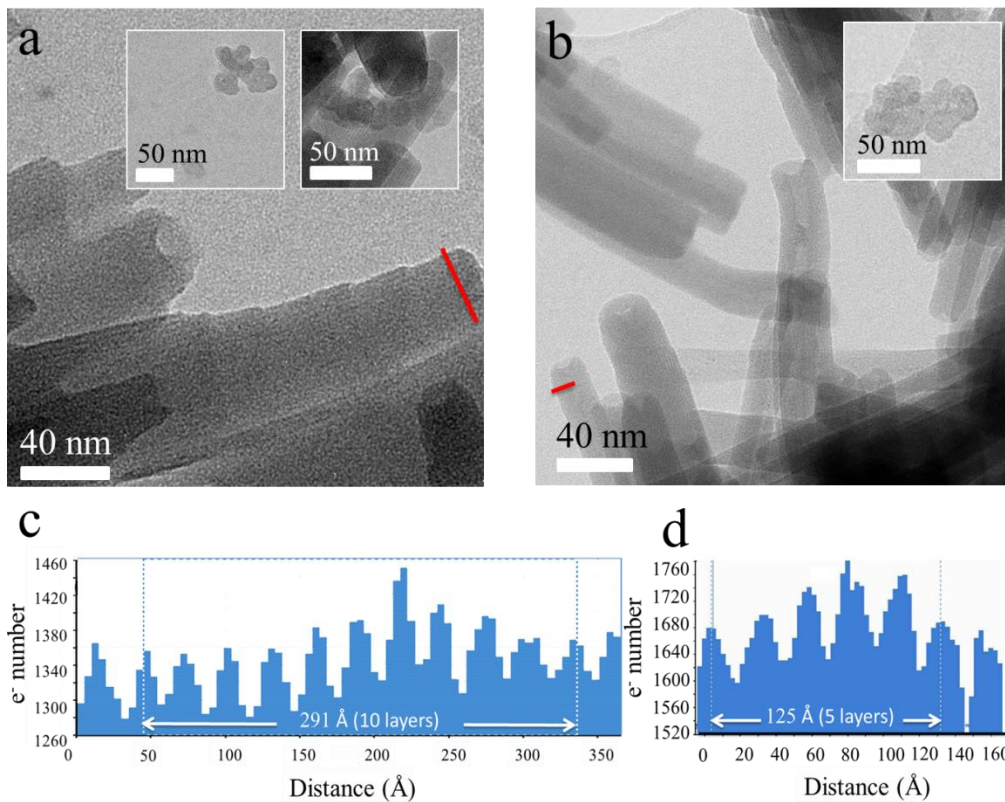


Figure S1. TEM micrographs of A_tGaS_x -NTs and A_tGaSe_y -NTs. Spherical particles, tens of nm in size with a hollow, layered structure, are observed as impurities in both cases (insets in a and b). Further studies of the structure and nature of these nanocages are ongoing. The intensity profiles taken along the nanotubes in the places indicated by a red line in (a) and (b) are shown in images (c) and (d), respectively. According to this, the layer separation is 29.1 Å for A_tGaS_x -NTs and 25.1 Å for the A_tGaSe_y -NTs.

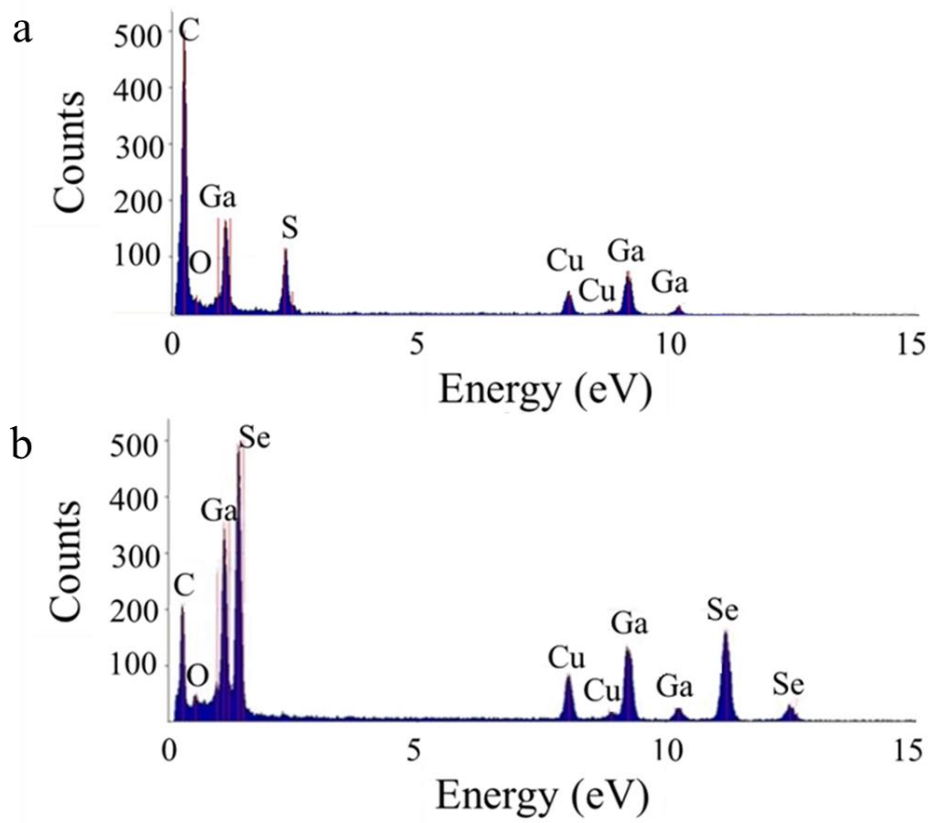
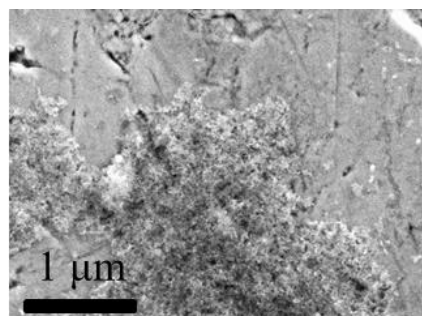
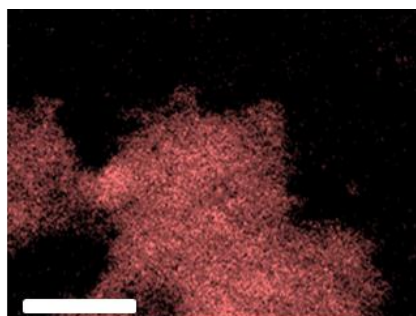


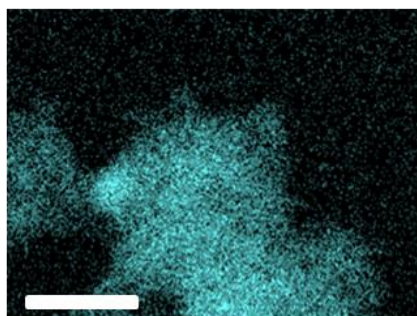
Figure S2. EDX (TEM) spectra of A_tGaS_x -NTs (a) and A_tGaSe_y -NTs (b). The copper signal comes from the holder.



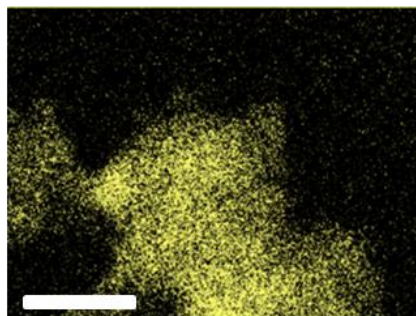
Electron Image



C K α



Ga K α



S K α

Figure S3. EDX mapping of the elements distribution on the A_tGaS_x -NTs performed on the SEM, showing the homogeneous distribution of carbon, gallium and sulfur in the nanotubes.

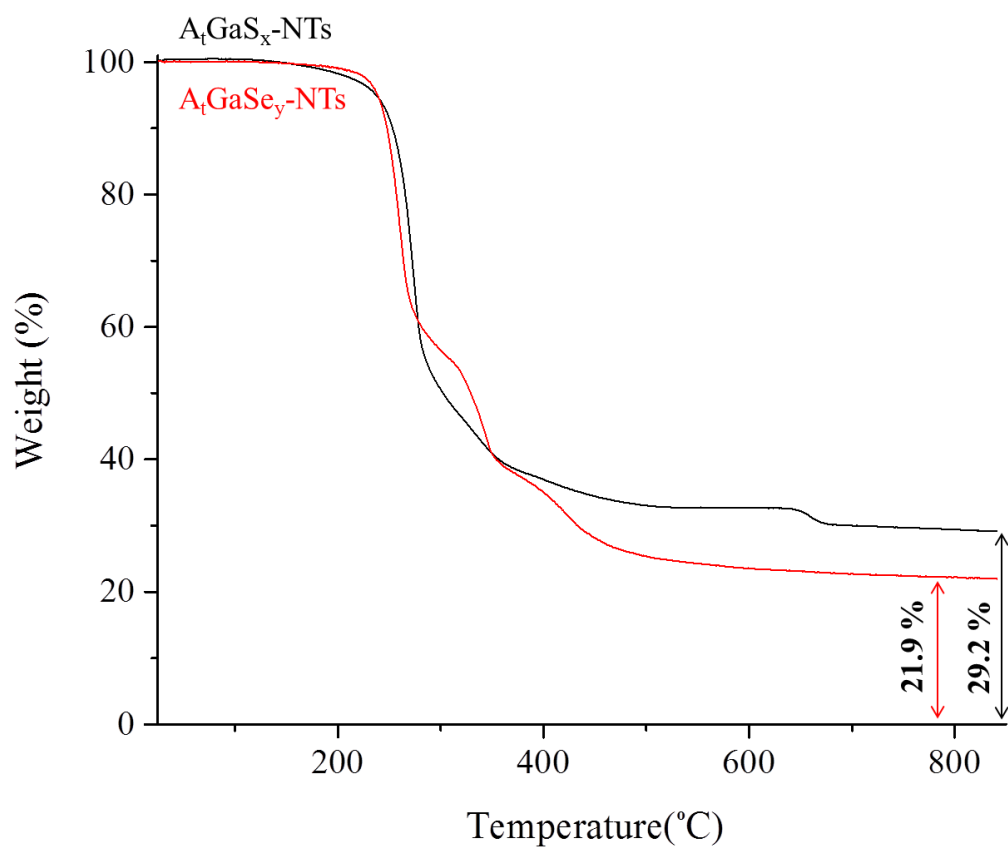


Figure S4. TGA curve of A_tGaS_x-NTs (black line) and A_tGaSe_y-NTs (red line). Heating rate was 10 °C/min, up to 850 °C, under air atmosphere.

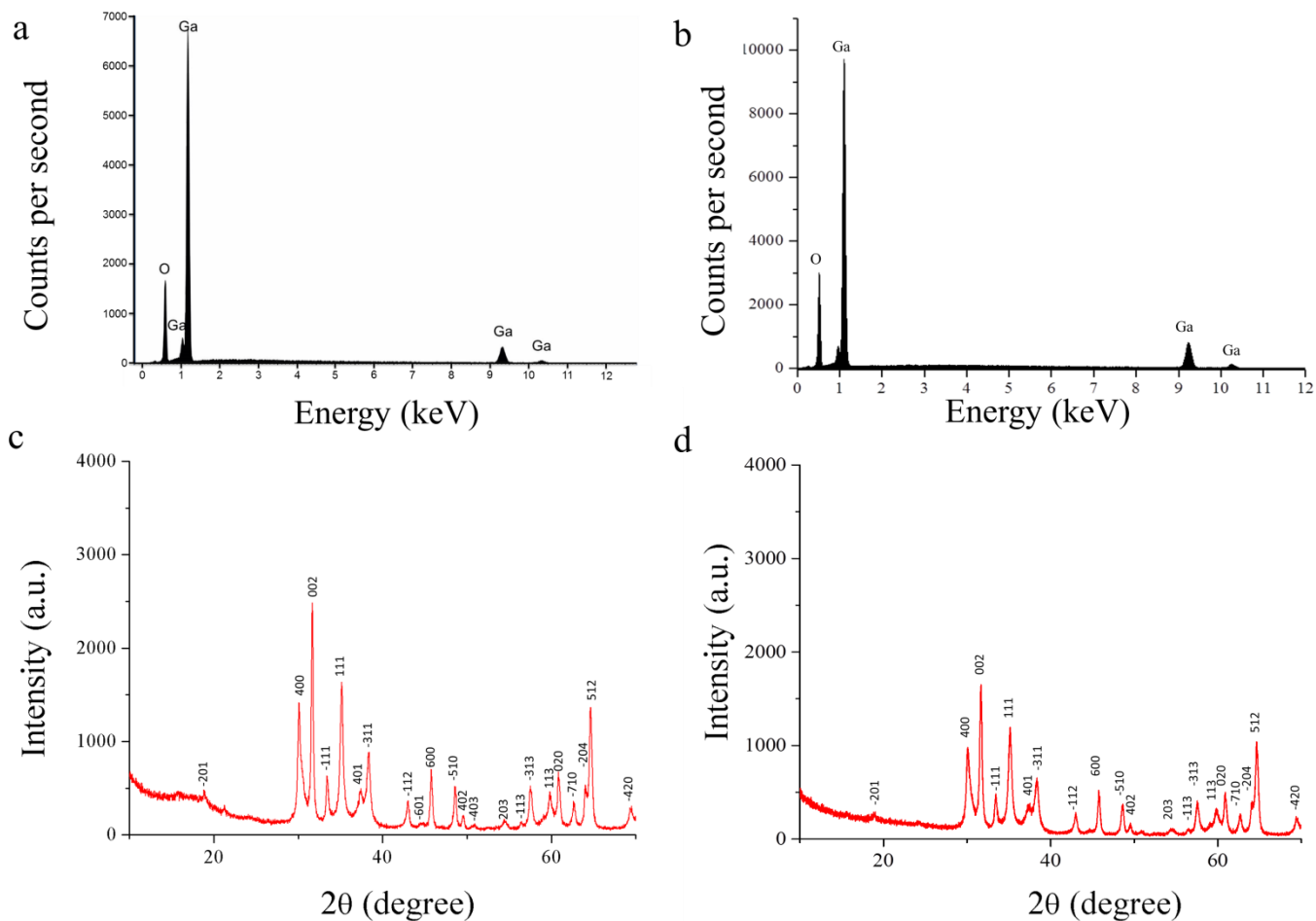


Figure S5. EDX (SEM) of the TGA residue of $A_t\text{GaS}_x\text{-NTs}$ (a) and $A_t\text{GaSe}_y\text{-NTs}$ (b), showing the presence of gallium and oxygen. TGA was performed under air atmosphere, and the samples were heated up to 850 °C. EDX measurements were performed in the SEM microscope using an acceleration voltage of 20 keV. XRD patterns of the TGA residues of $A_t\text{GaS}_x\text{-NTs}$ (c) and $A_t\text{GaSe}_y\text{-NTs}$ (d), showing the presence of monoclinic gallium (III) oxide in both cases.

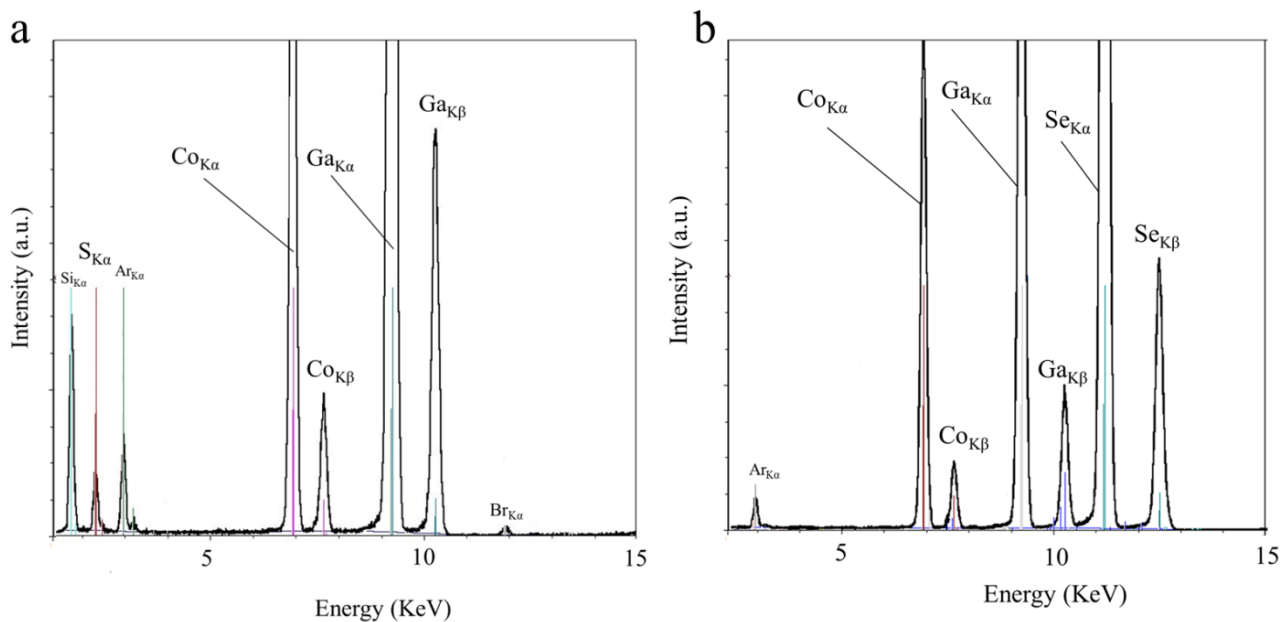


Figure S6. TXRF spectra of A₁GaS_x-NTs (a) and A₁GaSe_γ-NTs (b). The integration of area of the peaks after subtracting the background is proportional to the amount of the elements in the sample. Bromine is observed as a minor contaminant in sample (a). The argon signal comes from the inert atmosphere used during the measurements. Samples were prepared by dispersing the nanotubes in isopropyl alcohol by mild sonication. Cobalt was used as an internal standard, with a concentration of 100 μg/cm³. An aliquot was deposited on a quartz sample carrier and analyzed by TXRF.

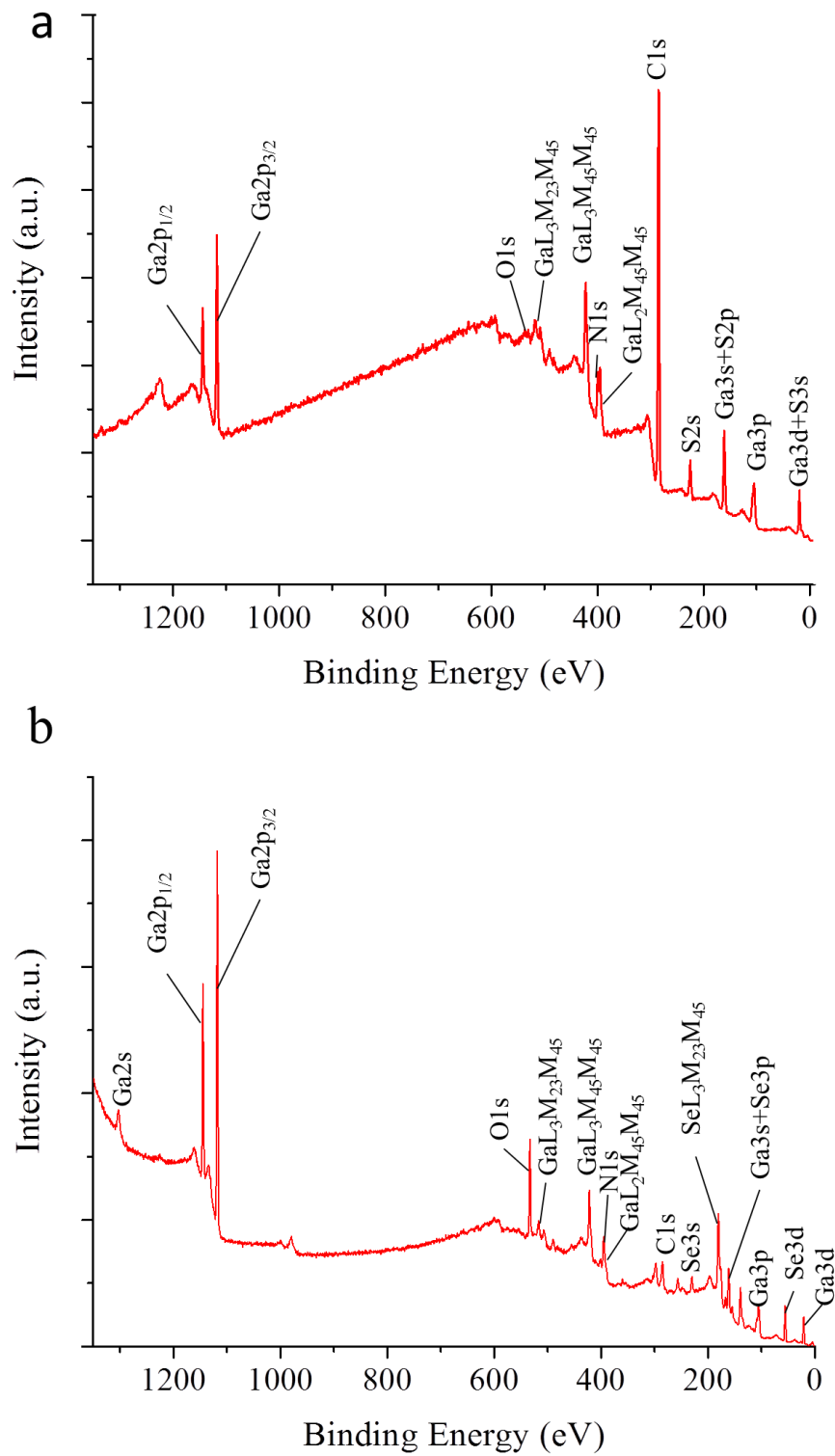


Figure S7. XPS survey of A_tGaS_x -NTs, showing the presence of gallium, sulfur, carbon, nitrogen and oxygen (a). XPS survey of A_tGaSe_y -NTs, showing a composition of gallium, selenium, carbon, nitrogen and oxygen (b).

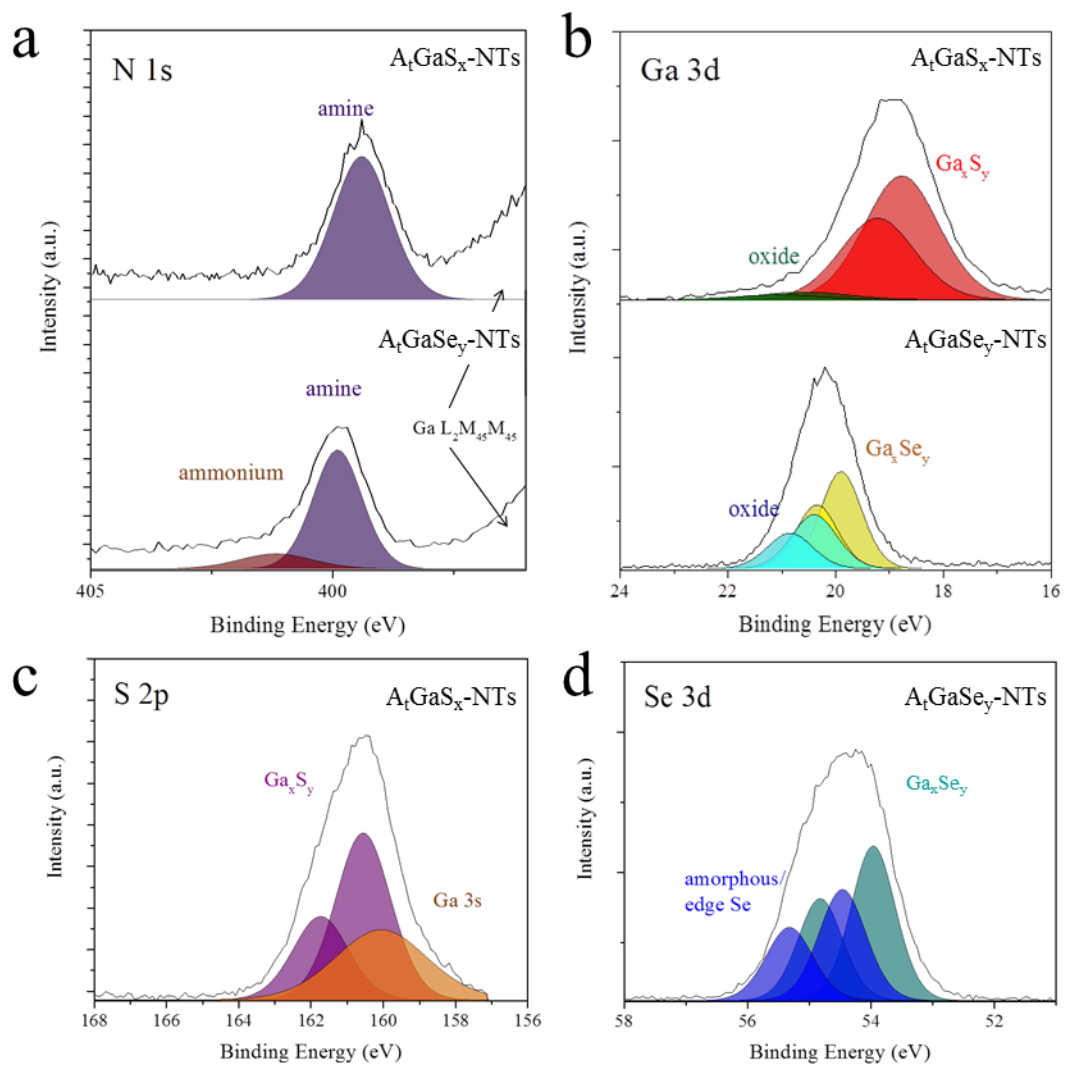


Figure S8. XPS of N1s (a), Ga3d (b), S2p (c) and Se3d (d) regions of A_tGaS_x-NTs and A_tGaSe_y-NTs .

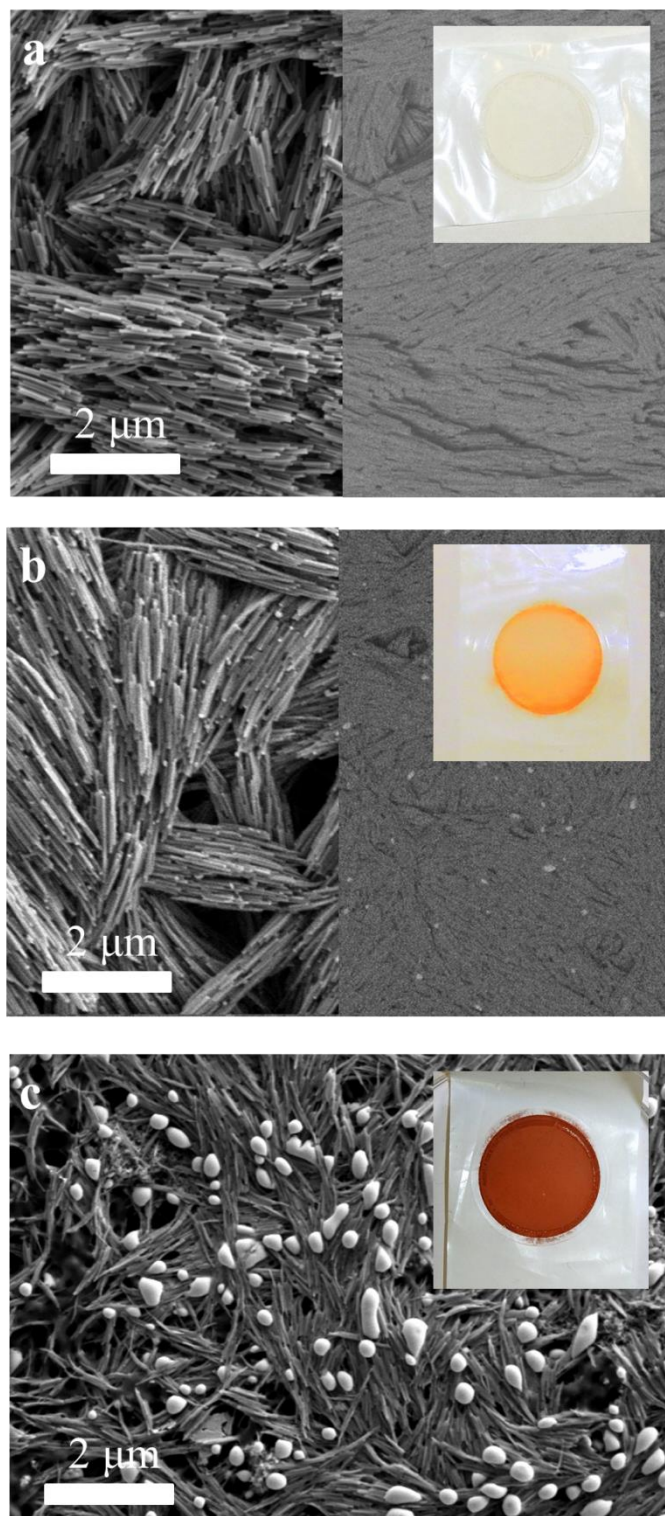


Figure S9. SEM images illustrating the ageing of A_tGaSe_y -NTs: fresh sample (a), sample aged for 1 day (b) and 1 week (c) under air atmosphere. The right side in images (a) and (b) were acquired using a backscattered electrons detector to better illustrate the nanoparticle formation.

1- Description of the optimization synthesis of the amine-templated gallium chalcogenide nanotubes

1.1- Amine-templated gallium sulfide nanotubes (A_1GaS_x -NTs)

1 mmol of $Ga(acac)_3$ and 1 mmol of sulfur were reacted at different temperatures for 144 h (150–250 °C at intervals of 25 °C, Table 1 in ESI[†], samples A–E). A colour change from pale yellow to transparent, and the subsequent formation of a white precipitate, was observed at 175 and 200 °C, whereas no changes were discernible outside this temperature interval.

These results indicate the existence of a range of temperatures where the synthesis is feasible, in accordance to the thermal decomposition/sublimation temperature of $Ga(acac)_3$.¹ The upper synthesis temperature is defined by the thermal stability of the white precipitate, which is re-dissolved by increasing the temperature above 220 °C. No reaction was observed at 150 °C, probably due to slow kinetics.

SEM characterization reveals that the morphology of the materials depends on the synthesis temperature. As shown in Figure 1a, tubular, hollow structures with lengths of 100–500 nm and diameters of tens of nanometres are obtained at 200 °C, whereas spheres with lateral dimensions of several micrometres and composed of intergrown fibrillar particles are produced at 175 °C (Figure S10a and b in ESI[†]). To improve the quality and yield of the tubular structures, the temperature was set to 200 °C in later experiments.

Following, the effect of the precursors molar ratio on the structure and yield of the obtained materials was studied, for which the initial gallium to sulfur stoichiometries were adjusted to 1:1, 1:1.5 and 1:2 (Table 1 in ESI[†], samples C, F and G, respectively). SEM images of the products obtained at ratios of 1:1.5 and 1:2 (Figure S10d and e in ESI[†]) show a similar nanotubular structure to that obtained when a ratio 1:1 is used.

When using gallium to sulfur ratios higher than 1:1, the yield of the reaction dramatically increases. In addition, the time required until the formation of the white precipitate depends on the gallium to sulfur starting ratios: 72 h, 24 h and 2 h when using ratios of 1:1, 1:1.5 and 1:2, respectively. Note that the total reaction time is 144 h in the three cases. Thus, a gallium to sulfur ratio of 1:2 was selected to maximize the yield of the reaction.

The optimum reaction time was defined by measuring the amount of precipitate yielded after 6, 12, 24, 72 and 144 h (Table 1, samples H, I, J, K and G, respectively). The maximum amount of nanotubes was reached after 24 h (reaction completion was confirmed by SEM). However, the nanotubes

synthesized after 72 h (Figure 1a) show a higher aspect ratio than those produced at 24 h (Figure S10e in ESI[†]), so 72 h was set as the optimum time.

To determine the utility of different precursors, alternative sulfur precursors, including diphenyldisulfide (Ph_2S_2), diisopropyldisulfide (iPr_2S_2) and dibenzoyldisulfide (Bz_2S_2) (Table 1 in ESI[†], samples L–N, respectively), were explored in the synthesis of the nanotubes. These chemicals were purchased from Sigma-Aldrich with purities higher than 96 % and used as received. In these reactions, 1 mmol of $\text{Ga}(\text{acac})_3$ was reacted with 1 mmol of R_2S_2 ($\text{R} = \text{iPr}, \text{Ph}, \text{Bz}$). Nanotubes were only obtained when using Bz_2S_2 as a precursor (Figure S10f in ESI[†]), demonstrating that, in addition to elemental sulfur, this compound is a valid precursor for the synthesis of the nanotubes.

The reactivity of disulfides towards the formation of metal sulfides follows the trend $\text{Bz}_2\text{S}_2 > \text{iPr}_2\text{S}_2 > \text{Ph}_2\text{S}_2$.² In the present study, only Bz_2S_2 seems to be reactive enough to produce nanotubes under the reaction conditions. However, due to the lower reaction yield in this case (Table 1), in addition to the higher size distribution of the nanotubes observed by SEM (Figure S10f in ESI[†]), sulfur was maintained as the preferred precursor.

In summary, the optimum parameters for the synthesis of $\text{A}_t\text{GaS}_x\text{-NTs}$ are $\text{Ga}(\text{acac})_3$ and sulfur as precursors, in molar ratio 1:2, reacting for 72 h at 200 °C.

Table 1. Optimization of the synthesis conditions of A_tGaS_x -NTs: temperature study (samples A-E), gallium to sulfur molar ratio study (samples C, F and G), time optimization (samples G and H-K) and study of disulfides as alternative sulfur precursors (samples L-N). 1 mmol of $Ga(acac)_3$ was utilized as gallium precursor in all reactions and a mixture of 100 mmol of hexadecylamine and 20 mmol of dodecylamine was used as solvent. *Yield is calculated with respect to gallium, based on the starting $Ga(acac)_3$ amount and the gallium content in the tubes calculated from TGA results.

Sample	Sulfur precursor	Temperature (°C)	Ga/S molar ratio	Reaction time (h)	Yield* (%)
A	Sulfur	150	1:1	144	-
B	Sulfur	175	1:1	144	n.a.
C	Sulfur	200	1:1	144	1.0
D	Sulfur	225	1:1	144	-
E	Sulfur	250	1:1	144	-
F	Sulfur	200	1:1.5	144	62.0
G	Sulfur	200	1:2	144	70.4
H	Sulfur	200	1:2	6	55.2
I	Sulfur	200	1:2	12	64.4
J	Sulfur	200	1:2	24	70.8
K	Sulfur	200	1:2	72	69.2
L	Ph₂S₂	200	1:2	144	-
M	iPr₂S₂	200	1:2	144	-
N	Bz₂S₂	200	1:2	144	46.5

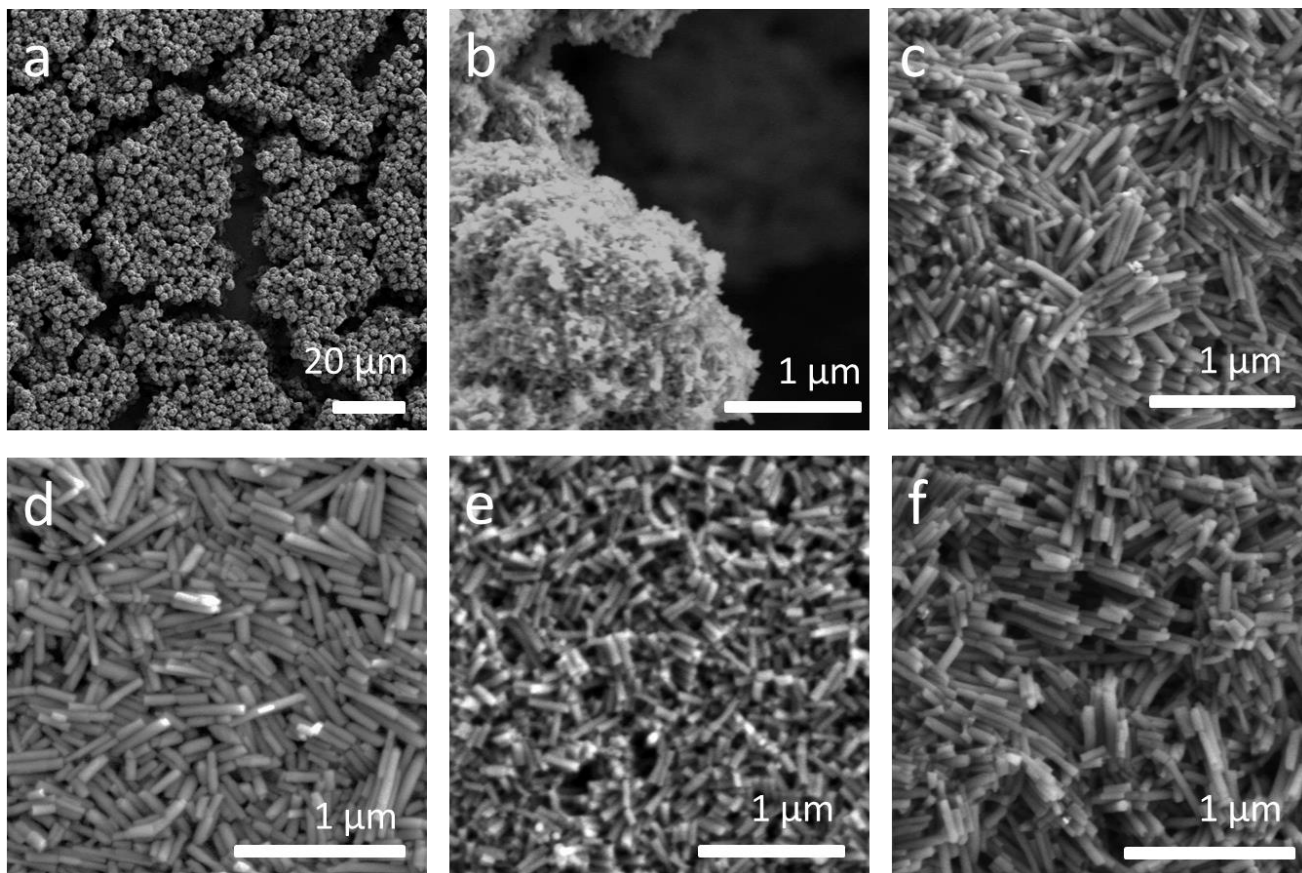


Figure S10. SEM micrographs of A_lGaS_x -NTs: intergrown nanotubes synthesized at 175 °C (a, b), nanotubes synthesized using a gallium to sulfur ratio of 1:1.5 (c) and 1:2 (d), nanotubes synthesized during time study, after 24 h (e) and nanotubes synthesized using Bz_2S_2 as sulfur precursor (f).

1.2- Amine-templated gallium selenide nanotubes (A_1GaSe_y -NTs)

A similar procedure as described above was utilized to optimize the synthesis of A_1GaSe_y -NTs (Table 2 in ESI[†]). In this case, the formation of a white precipitate was observed at temperatures of 175, 200 and 225 °C (samples P, Q and R), showing that the range of temperatures for the feasible synthesis of the nanotubes is broader than in the case of the sulfur. Nanotubes synthesized at 175 °C (Figure S11a in ESI[†]) show a smaller size than those prepared at 200 °C (Figure S11b in ESI[†]), which indicates that the average size of the nanotubes can be tuned by controlling the synthesis temperature. Moreover, SEM of the sample synthesized at 225 °C shows a high number of impurities (Figure S11c in ESI[†]). Thus, 200 °C was selected as optimum synthesis temperature in order to maximize the size and quality of the nanotubes.

Nanotubes produced at gallium:selenium starting ratios higher than 1:1 showed a high increase in the amount of material obtained (see Table 2 in ESI[†], samples Q, T and U). In this case, the yield when using ratios of 1:1.5 (Figure S11d in ESI[†]) and 1:2 (Figure S11e in ESI[†]) was similar, so the ratio 1:1.5 was selected in order to minimize the usage of selenium precursor.

The time study of the reaction (Table 2, samples T, V-Y) shows that the nanotubes can be isolated after 24 h of reaction (Figure S11f in ESI[†]), reaching the maximum yield after 72 h. SEM confirmed the similar morphology of nanotubes synthesized after 72 and 144 h of reaction.

Diphenyldiselenide (Ph_2Se_2) and dibenzylidiselelenide (Bz_2Se_2) were purchased from Sigma Aldrich and used as received. These compounds were explored as alternative selenium precursors for the synthesis of the nanotubes (Table 2 in ESI[†], samples Z and AA). However, the formation of a precipitate was not observed, which indicated that the reactivity of the diselenides is not high enough to produce the nanotubes or other compounds at 200 °C, and no further experiments were carried out with these precursors.

In summary, the optimized conditions for the synthesis of A_1GaSe_y -NTs are 200 °C during 72 h, using $Ga(Acac)_3$ and selenium as precursors, in a molar ratio 1:1.5.

Table 2. Synthesis conditions optimization of the A_tGaSe_y -NTs: temperature study (samples O-S), gallium to selenium molar ratio study (samples Q, T and U), time optimization (samples T and V-Y) and study of diselenides as alternative selenium precursors (samples Z, AA). 1 mmol of $Ga(acac)_3$ was utilized as gallium precursor in all reactions and a mixture of 100 mmol of hexadecylamine and 20 mmol of dodecylamine was used as solvent. *Yield is calculated with respect to gallium, based on the starting $Ga(acac)_3$ amount and the gallium content in the tubes calculated from TGA results.

Sample	Selenium precursor	Temperature (°C)	Ga/Se molar ratio	Reaction time (h)	Yield* (%)
O	Selenium	150	1:1	144	-
P	Selenium	175	1:1	144	16.7
Q	Selenium	200	1:1	144	27.2
R	Selenium	225	1:1	144	32.2
S	Selenium	250	1:1	144	-
T	Selenium	200	1:1.5	144	74.0
U	Selenium	200	1:2	144	75.1
V	Selenium	200	1:1.5	12	1.2
W	Selenium	200	1:1.5	24	58.4
X	Selenium	200	1:1.5	72	72.8
Y	Selenium	200	1:1.5	120	73.9
Z	Ph₂Se₂	200	1:1.5	144	-
AA	Bz₂Se₂	200	1:1.5	144	-

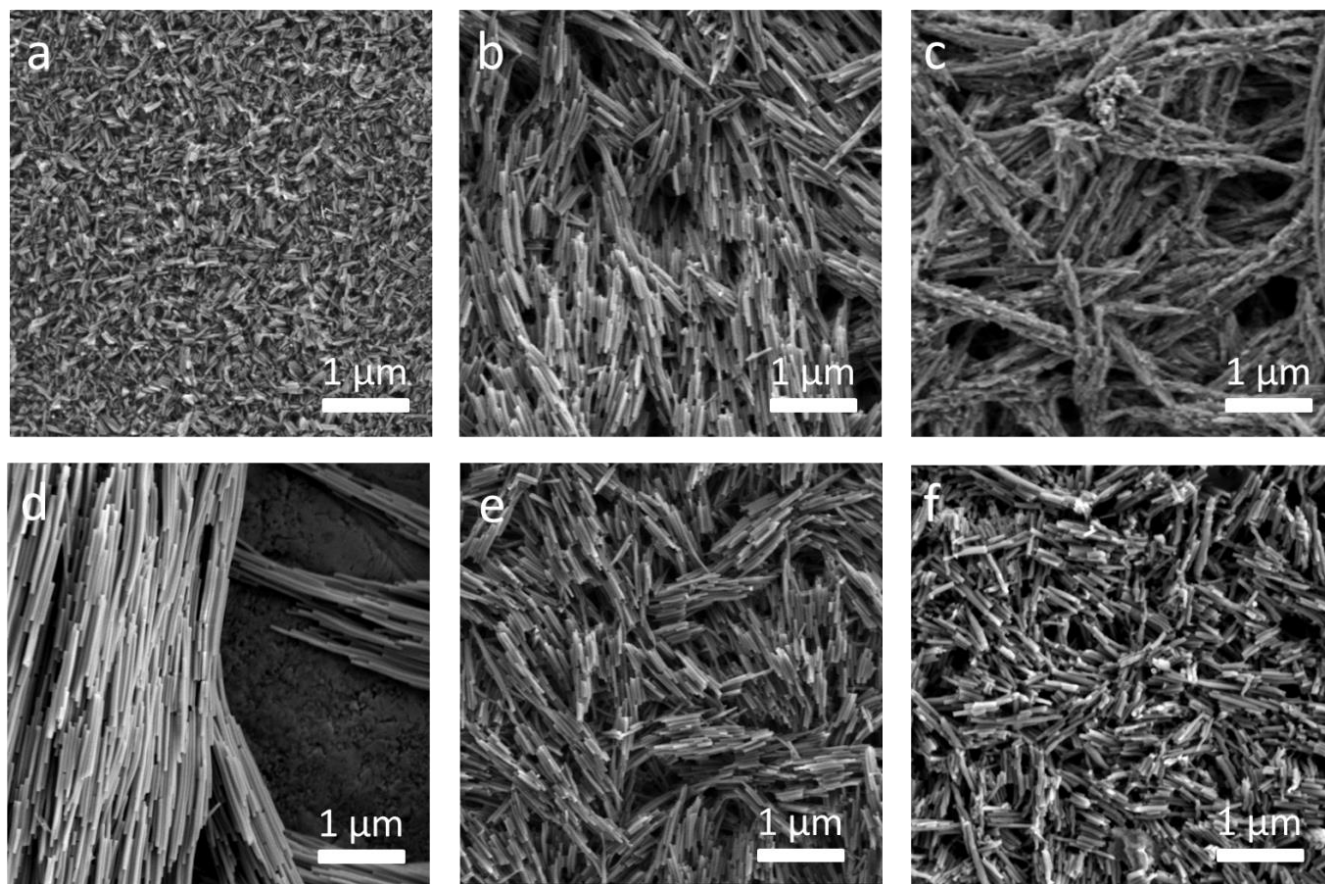


Figure S11. SEM micrographs of A_tGaSe_y -NTs: nanotubes synthesized at 175 °C (a), 200 °C (b) and 225 °C (c), nanotubes synthesized using a gallium to sulfur ratio of 1:1.5 (d) and 1:2 (e) and nanotubes synthesized during time study, after 24 h (f).

1.3- Amine-templated gallium telluride nanotubes synthesis studies

The preparation of amine-templated gallium telluride nanotubes was attempted. However, the synthesis was not feasible in similar conditions to those described for sulfur and selenium (Table 3 in ESI[†]). Reactions performed between Ga(acac)₃ and tellurium (BB to HH) did not show the formation of any precipitate. Differently from sulfur and selenium, tellurium was not observed to dissolve in the mixture of amines in the range of temperatures studied, and SEM of the solid isolated after the reaction showed only the presence of an amorphous solid identified as unreacted tellurium by EDX (Figure S12a and c in ESI[†]).

When dibenzyltelluride (Bz₂Te₂) (98%, Sigma Aldrich) was used as tellurium precursor, no solid could be isolated from reactions performed at temperatures below 240 °C, yielding only polyhedral and needlelike micron-sized particles at temperatures in the range of 240 to 300 °C (Figure S12b in ESI[†]), identified as trigonal tellurium by XRD (Figure S12d in ESI[†]). These results are similar to the previously reported synthesis of micro-tubular tellurium crystals.³ These results showed that the amine-templated gallium telluride nanotubes could not be produced by this synthesis method. Further experiments to prepare these materials by a different approach are ongoing.

Table 3. Synthesis conditions in the gallium-tellurium system: temperature study (samples BB-FF), gallium to tellurium molar ratio study (samples DD, GG and HH), and study of ditellurides as alternative tellurium precursor at different temperatures (samples II-NN). 1 mmol of Ga(acac)₃ was utilized as gallium precursor in all reactions and a mixture of 100 mmol of hexadecylamine and 20 mmol of dodecylamine was used as solvent. Reaction time was 144 h in all cases.

Sample	Tellurium precursor	Temperature (°C)	Ga/Te molar ratio
BB	Tellurium	150	1:1
CC	Tellurium	175	1:1
DD	Tellurium	200	1:1
EE	Tellurium	225	1:1
FF	Tellurium	250	1:1
GG	Tellurium	200	1:1.5
HH	Tellurium	200	1:2
II	Bz ₂ Te ₂	200	1:2
JJ	Bz ₂ Te ₂	220	1:2
KK	Bz ₂ Te ₂	230	1:2
LL	Bz ₂ Te ₂	240	1:2
MM	Bz ₂ Te ₂	265	1:2
NN	Bz ₂ Te ₂	300	1:2

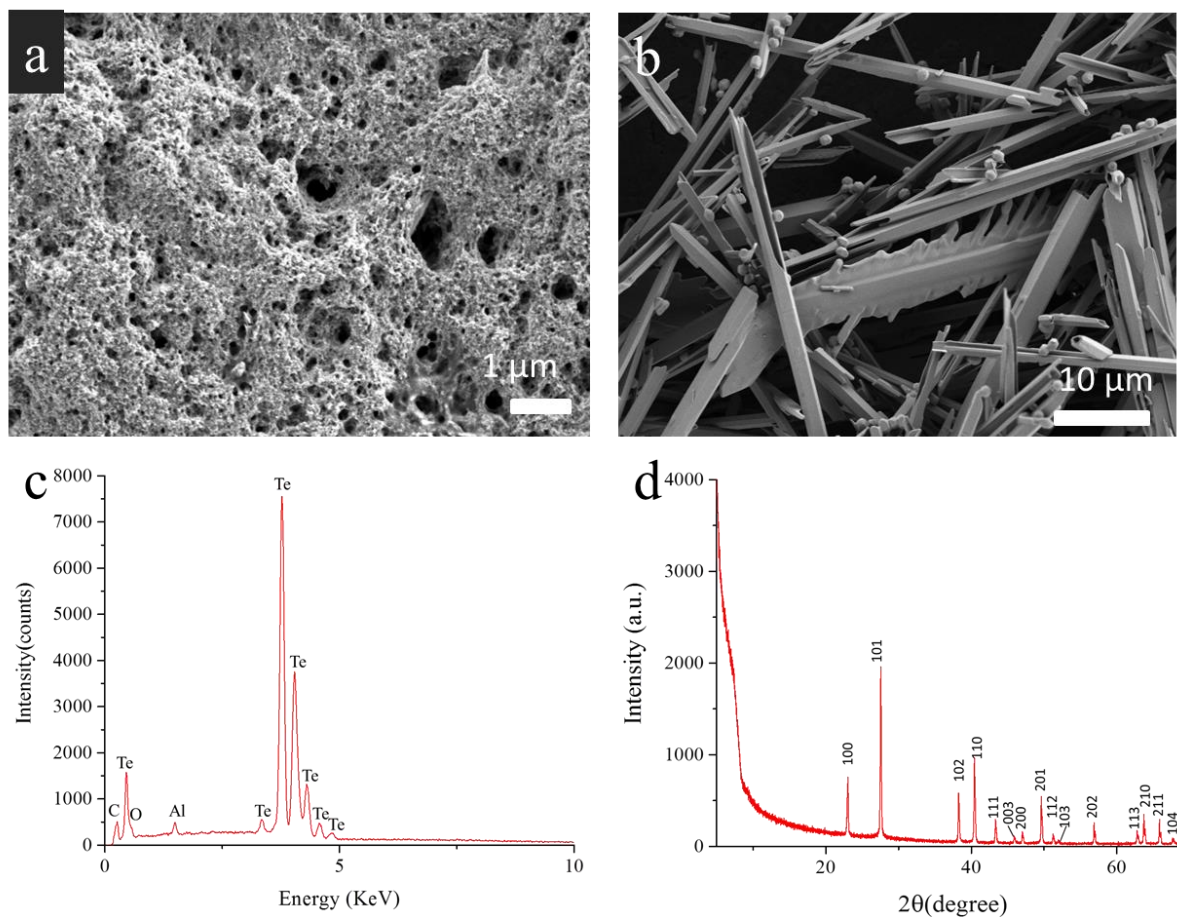


Figure S12. SEM micrograph of sample DD, showing an amorphous morphology (a), and micrograph of the micron-sized particles obtained when using Bz₂Te₂ as precursor, in reaction LL (b). EDX analysis of sample DD, shown in (c), confirms the absence of gallium in the amorphous powder and its tellurium-based composition. Aluminum and oxygen signals come from the holder, and carbon signal from impurities from the solvent. XRD of sample LL, shown in (d), indicates that the material is composed of trigonal tellurium.

3- References

1. R. M. Mahfouz, K. M. Al-Khamis, M. R. H. Siddiqui, N. S. Al-Hokbany, I. Warad and N. M. Al-Andis, *Prog React Kinet Mec*, 2012, **37**, 249-262.
2. S. R. Alvarado, Y. J. Guo, T. P. A. Ruberu, E. Tavasoli and J. Vela, *Coordin Chem Rev*, 2014, **263**, 182-196.
3. J. Lu, Y. Xie, F. Xu and L. Y. Zhu, *J Mater Chem*, 2002, **12**, 2755-2761.